Virology 441 (2013) 75–84

Contents lists available at SciVerse ScienceDirect

Virology

journal homepage: www.elsevier.com/locate/yviro

Characterization of the guinea pig CMV gH/gL/GP129/GP131/GP133 complex in infection and spread

Marcy Auerbach [a], Donghong Yan [b], Ashley Fouts [a], Min Xu [b], Alberto Estevez [c], Cary D. Austin [d], Fernando Bazan [e], Becket Feierbach [a,*]

[a] Department of Infectious Diseases, Genentech, Inc./Hoffmann-LaRoche, Ltd., 1 DNA Way, South San Francisco, CA 94080, United States
[b] Department of Translational Immunology, Genentech, Inc./Hoffmann-LaRoche, Ltd., 1 DNA Way, South San Francisco, CA 94080, United States
[c] Baculovirus expression group, Genentech, Inc./Hoffmann-LaRoche, Ltd., 1 DNA Way, South San Francisco, CA 94080, United States
[d] Department of Pathology, Genentech, Inc./Hoffmann-LaRoche, Ltd., 1 DNA Way, South San Francisco, CA 94080, United States
[e] 4th & Aspen Life Sciences Consulting LLC, 924 4th St. N Stillwater, MN 55082, USA

ARTICLE INFO

Article history:
Received 30 July 2012
Returned to author for revisions
15 February 2013
Accepted 13 March 2013
Available online 4 April 2013

Keywords:
Cytomegalovirus
Congenital infection
Viral entry
Animal model

ABSTRACT

In human cytomegalovirus (HCMV), the UL128-131A locus plays an essential role in cellular tropism and spread. Here, we report the complete annotation of the GP129-133 locus from guinea pig cytomegalovirus (GPCMV) and the discovery of the UL131A homolog, named GP133. We have found that similar to HCMV the GP129-133 proteins form a pentamer complex with the GPCMV glycoproteins gH and gL. In addition, we find that the GP129-133 proteins play a critical role in entry as the GP129-133 deletion mutant shows a defect in both endothelial and fibroblast cell entry. Although the GP129-133 deletion strain can propagate in vitro, we find that the deletion fails to spread in vivo. Interestingly, the wildtype strain can spontaneously give rise to the GP129-133 deletion strain during in vivo spread, suggesting genetic instability at this locus.

Introduction

Herpesviruses are prevalent animal pathogens, producing a variety of medical illness and disease. Human cytomegalovirus (HCMV, species Human herpesvirus 5) is the most common cause of congenital virus infection. Congenital HCMV infection occurs in 0.2–1% of all births, and causes birth defects and developmental abnormalities, including sensorineural hearing loss (SHNL) and developmental delay (Ogawa et al., 2007; Pass, 2002). Animal models are often valuable for understanding pathogenesis and for developing therapies for infectious disease, and in the case of CMV, models are particularly necessary since the species-specificity precludes the study of HCMV in laboratory animals (Powers and Fruh, 2008; Schleiss, 2002). In contrast to murine CMV (MCMV) and rat CMV (RCMV), guinea pig CMV (GPCMV) crosses the placenta and causes infection *in utero* (Schleiss, 2002). This makes the GPCMV animal model useful for studies on transplacental transmission of CMV and vaccine development (Schleiss, 2006, 2007). The only commercially-available GPCMV strain (strain 22122 from the American Type Culture Collection) was revealed to be a mixture of two variants: one containing a wildtype 1.6 kb locus encoding the homologs of HCMV UL128 and UL130, GP129 and GP131, respectively, and the other containing a deletion of this region (Nozawa et al., 2008). A homolog of HCMV UL131A has not been described. The 1.6 kb locus was shown to be required for efficient viral growth in animals, but dispensable for growth in cell culture (Nozawa et al., 2008). However, conclusions from these prior studies are limited due to the lack of guinea pig-specific reagents, such as primary cell lines and antibodies to the proteins encoded by this locus.

The HCMV gH/gL/UL128/UL130/UL131A complex is required for viral entry into epithelial cells, endothelial cells, and macrophages, but not fibroblasts, and is a major antigen of the human neutralizing immune response (Fouts et al., 2012; Hahn et al., 2004; Wang et al., 2011; Wang and Shenk, 2005a, 2005b). It is well known that propagation of HCMV in fibroblasts leads to the instability and functional loss of the UL128-131A complex (Hahn et al., 2004; Wang and Shenk, 2005a, 2005b). The HCMV UL128, UL130, and UL131A proteins form a pentameric complex with glycoprotein H (gH) and glycoprotein gL (gL) (Ryckman et al., 2008). gH and gL have been identified in GPCMV, but it is unknown if these proteins form a heterodimer (Brady and Schleiss, 1996; Paglino et al., 1999). Furthermore, it is unknown if gH and gL form an analogous complex with the aforementioned GP129 and GP131.

In this study, we have confirmed the expression of GP133 and identified it as a homolog of HCMV UL131A. In addition, we show that GP133 can form a pentameric complex with GPCMV gH, gL,

* Correspondence to: Department of Infectious Diseases, Genentech, Inc./Hoffmann-LaRoche, Ltd., 1 DNA Way, Building 11, MS 33, South San Francisco, CA 94080, United States. Fax: +1 650 225 6103.
E-mail address: becketf@gene.com (B. Feierbach).

0042-6822/$ - see front matter © 2013 Elsevier Inc. All rights reserved.
http://dx.doi.org/10.1016/j.virol.2013.03.008

GP129, and GP131. Using guinea pig-derived primary endothelial and fibroblast cell lines, we demonstrate that the GP129-133 locus serves a role in viral entry into cells. Furthermore, we have found that, the GP129-133 locus is genetically unstable in vivo leading to a mixture of wildtype and a mutant with a deletion of this region.

Results

Assay and primary cell development for the study of GPCMV

The gold standard for titering GPCMV is the $TCID_{50}$ assay and the plaque assay. These methods, however tried and true, involve lengthy read-outs and are cell-culture reagent intensive. We sought to develop an alternative immunofluorescence assay (IFA), similar to that utilized for HCMV. We found that an anti-GPCMV glycoprotein B monoclonal antibody (29-29) produced strong, specific anti-viral staining. Although HCMV gB is characterized as a late protein, we have been able to detect robust expression in infected cells at 24 hpi by Western blot (data not shown) and by immunofluorescence (Fig. 1A)(Britt and Harrison, 1994; Spaete et al., 1988). Although we observed greater staining at 48 hpi, the percent of cells infected at 24 hpi corresponded to the input inoculum as determined by $TCID_{50}$. Moreover, we could detect spread at 48 hpi, as defined by >2 contiguous cells infected, but not at 24 hpi, suggesting that we are visualizing primary infection at 24 hpi (Fig. 1A). When the viral inoculum was UV-treated prior to infection, we did not detect anti-gB staining, indicating that the cytoplasmic staining is the result of replicated virus (Fig. 1B). IFA was additionally used as readout for a GPCMV neutralization assay.

Studies concerning GPCMV cell entry have been hampered by the lack of available guinea pig primary cells. There are only two commercially available guinea pig cell lines and we deemed both unsuitable for this study (guinea pig lung fibroblast cell line, ATCC CCL-158, gives rise to cultures with heterogeneous morphology, and guinea pig epithelial cell line, ATCC CCL-242, is non-permissive for GPCMV). In an effort to generate cells that are relevant, characterized, and permissive to GPCMV infection, we isolated fibroblasts from 40-day old guinea pig embryos and endothelial cells from adult guinea pig lungs and aortas and sorted both tissues with the endothelial cell marker CD31/PECAM-1 (Conner, 2001; Kobayashi et al., 2005). To characterize these cells, we generated a panel of fibroblast- and endothelial-specific markers for relative qRT-PCR (Supplemental Table 1). We based this panel on known markers for human and mouse fibroblast and endothelial cells and the availability of the guinea pig genome sequence (Garlanda and Dejana, 1997; Pilling et al., 2009). The qRT-PCR analysis demonstrated a clear enrichment of each cell-specific marker on the corresponding cell type (Supplemental Fig. 1). These primary cells were permissive to GPCMV as detected by cytopathic effect, IFA staining, and qPCR for the presence of a viral tegument gene (GP83) (Fig. 1A and data not shown). Due to the relevant nature of these cells, we chose to move forward with only primary cells in these studies.

Re-evaluation of the genomic landscape of the 1.6 kb locus

The glycoprotein complexes involved in the cellular entry of HCMV have been well characterized both biochemically and cell biologically. In contrast, the mechanisms regarding the entry of GPCMV are relatively unknown. To better understand the genomic landscape of the so-called “tropism” locus containing GP129 and GP131, we generated GPCMV cDNA from a pool of poly(A) RNA purified from GPCMV-infected cells and amplified the entire locus using primers based on the published genomic sequence

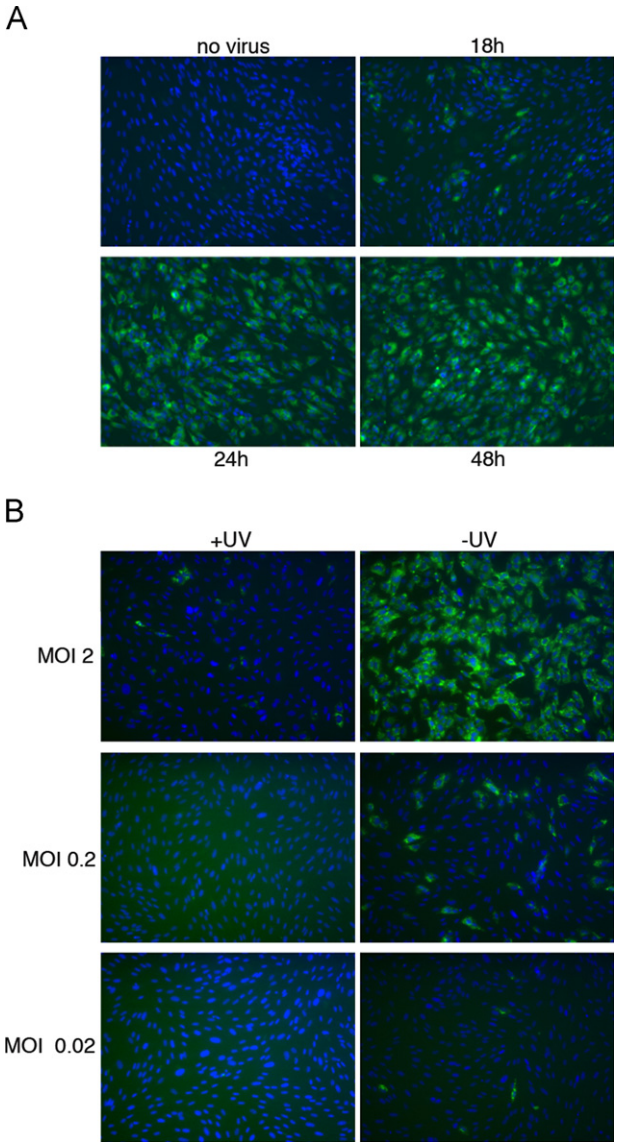

Fig. 1. Immunofluorescence of GPCMV-infected guinea pig-primary fibroblast cells. (A) Detection of gB using the anti-GPCMV gB monoclonal antibody, 29-29, during infection at 18, 24, and 48 h post-infection. Cells were infected at an MOI of 0.5. Antibody binding was detected with AlexaFluor 488 anti-mouse IgG secondary antibody (green) and nuclei were stained with DAPI (blue). Overlay images are shown. (B) GPCMV that was treated (left panel) or not treated (right panel) with UV. Three different MOIs are shown. Cells were fixed and stained at 24 h post-infection with the anti-gB antibody as described above.

encompassing the entire 1.6 kb region (Nozawa et al., 2008). The PCR reaction yielded three products that were individually cloned and sequenced. Two of the three products were incompletely spliced (i.e. contained introns in GP129 and GP131) and we moved forward with the cDNA that was completely spliced. As we did not follow up on the incompletely spliced products, we do not know if these products play a role in replication. Consistent with previous reports, we found that the GP129 and GP131 genes are found on the negative strand of the viral DNA genome, and that both genes are spliced, contain signal sequences, and lack transmembrane domains (Fig. 2A) (Kanai et al., 2011; Nozawa et al., 2008; Yamada et al., 2009). Both GP129 and GP131 sequences are identical to those published (Kanai et al., 2011; Nozawa et al., 2008).

Our analyses of these protein sequences revealed that GP129 and GP131 contain putative CC-type chemokine and CX-type chemokine motifs, respectively (Fig. 2A). Chemokine motifs are

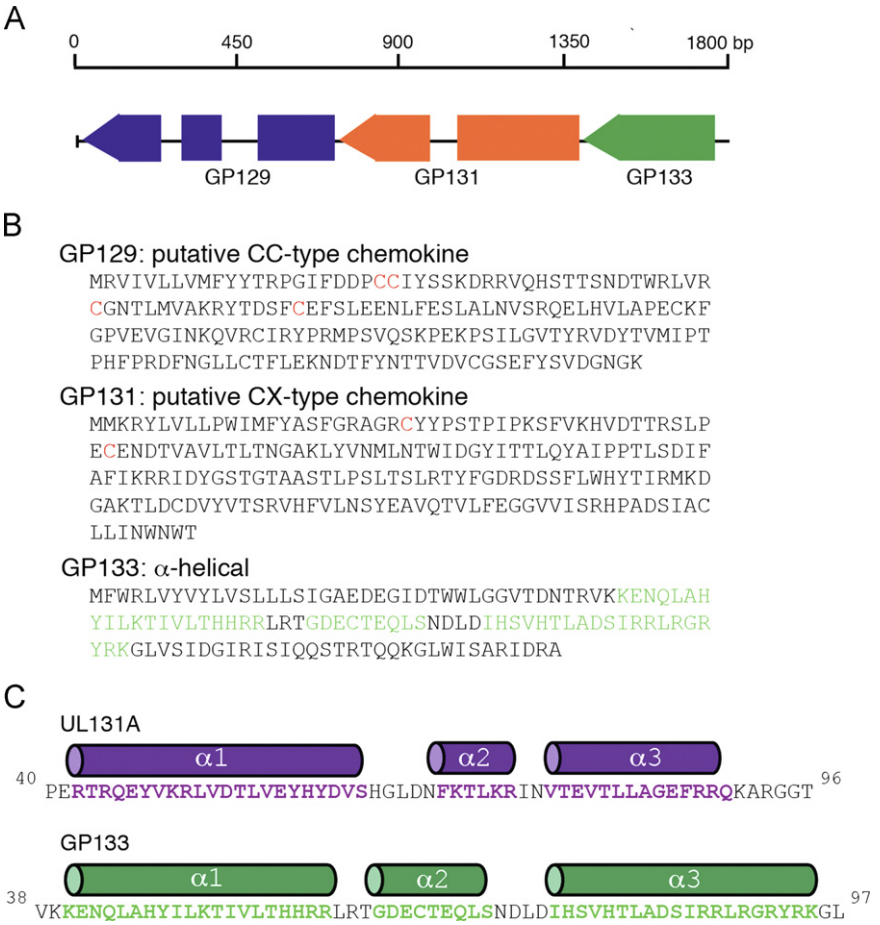

Fig. 2. Annotation of the GP129-133 locus. (A) Schematic of the GPCMV 129-133 locus with ORF designations and splice junctions shown. The locus is expressed from the Crick strand as a single mRNA. (B) Amino acid sequences of GP129, GP131, and GP133. Residues highlighted in red indicate cysteine residues that form putative chemokine folds and residues highlighted in green indicate predicted α-helicies for GP133. (C) Topological comparison of the predicted α-helical secondary structures in CCMV UL131A (purple) and GP133 (green). The relevant portion of the primary sequence is shown.

highly conserved at this locus and have been identified in MCMV, RCMV, CCMV and HCMV (Hahn et al., 2004). HCMV UL128 gene encodes a protein with a CC-type chemokine domain (Hahn et al., 2004). More recently, it was shown that soluble recombinant pUL128 was able to down-regulate host cell chemokine receptors and was sufficient to block migration of monocytes (Straschewski et al., 2011). GP129 has overall 48% amino acid similarity to UL128, and contains a CC-type motif at similar position in the amino acid sequence. Additionally, HCMV UL130 has been shown to be important for the infection of leukocytes (Hahn et al., 2004) and more recently has been described as containing a putative N-terminal CX-type chemokine motif (Malkowska et al., 2013; Wyrwicz and Rychlewski, 2007). The CX-type (also called C-type) motif involves only one cysteine bridge (instead of two) in a given chemokine fold. GP131 has overall 36% amino acid similarity to UL130, and contains a single putative CX-type motif at the N-terminus.

We confirmed the expression of a third gene, located 5′ of GP129 and GP131 on the cDNA, named GP133. This gene encoding a 127 amino acid protein was predicted by the initial annotation of this locus reported previously (Nozawa et al., 2008). GP133 is co-cistronic with GP129 and GP131, and its protein product is predicted to be largely alpha-helical in structure with three distinct alpha-helical domains, in which chimpanzee CMV (CCMV) UL131A contains the highest domain homology (32% similarity; Fig. 2B and C). Although the overall percentage amino acid similarity between GP133 and HCMV UL131A is low (29% similarity, 20% identity), we predict that GP133 is the homolog of UL131A due to the conserved protein domain architecture and syntenic position in the genome (Fig. 2C).

Characterization of GPCMV gH, gL, GP129, GP131, and GP133 proteins

To biochemically characterize the gH, gL, GP129, GP131, and GP133 proteins, we co-expressed all five proteins with C-terminal His tags in the baculovirus system. The transmembrane domain of gH was deleted to ensure soluble expression. Co-expressed proteins were purified over nickel resin and analyzed by Coomassie staining (data not shown) and Western blot (Fig. 3A). Bands for each of the five proteins were observed at the predicted molecular weights, as shown by the rabbit polyclonal anti-peptide antibodies (Fig. 3A). When we probed blots with a mouse anti-his antibody we were able to distinguish among the gH, GP131 and GP133 proteins, as these bands ran at the predicted molecular weights (Fig. 3A). However, gL and GP129 proteins co-migrate in SDS-PAGE and could not be distinguished using the anti-his antibody (Fig. 3A). Despite attempts to express these proteins in equal ratios, the anti-his Western blots show greater signal for gL and/or GP129, than gH, GP131, and GP133. It is possible that gL and/or GP129 are expressed in greater amounts or that the anti-his antibody recognizes gL and GP129 better due to accessibility. In any case, we cannot infer stoichiometry from these results. We also performed Western blot analysis on GPCMV-infected fibroblast cells (Fig. 3B). During infection, each component appeared to have slower migration, possibly due to modification such as glycosylation (Fig. 3B).

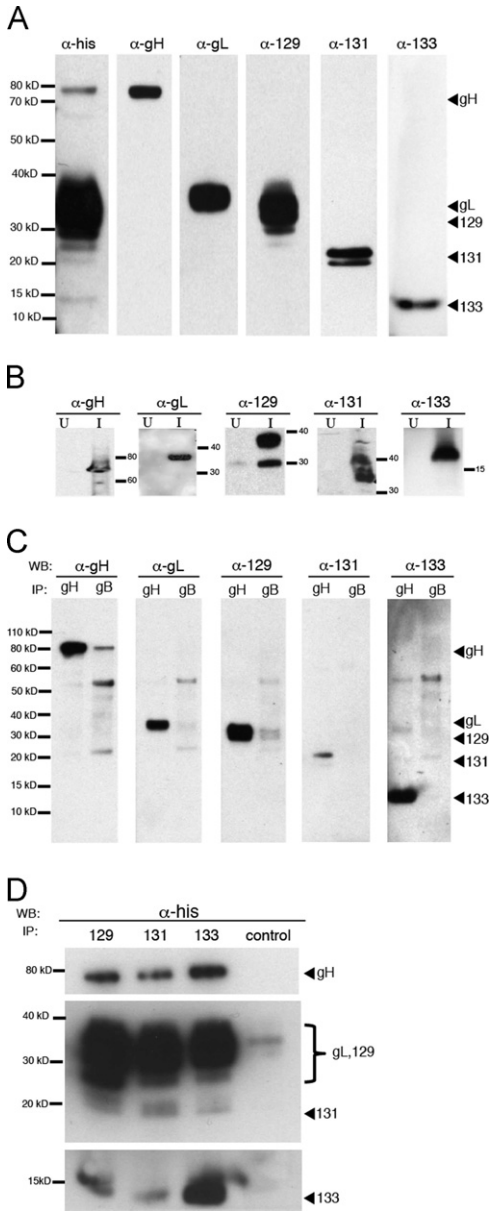

Fig. 3. Characterization of gH, gL, GP129, GP131, and GP133 and evidence of a pentameric complex. A–C, samples were run on a 4–12% gradient bis-Tris SDS-PAGE gel. (A) Co-expression of the soluble GPCMV gH/gL/GP129/GP131/GP133 in baculovirus. Western blot analysis using a mouse anti-his antibody and rabbit polyclonal antibodies against each protein and are shown. (B) Expression of GPCMV gH, gL, GP129, GP131, GP133 proteins in GPCMV-infected fibroblast cells. Comparison with uninfected cell lysates (U) is shown to the left of the infected cell lysates (I). Proteins were analyzed by immunoblotting with rabbit anti-peptide antibodies directed against each protein. (C) Co-immunoprecipations of the baculovirus-derived GPCMV gH, gL, GP129, GP131, GP133 proteins were performed with an anti-GPCMV gH antibody (mAb 394) or with a species control antibody against GPCMV gB (29-29). Immunoprecipitations were followed by SDS-PAGE/Western blot using rabbit polyclonal antibodies against each protein. (D) Co-immunoprecipations of the baculovirus-derived GPCMV gH, gL, GP129, GP131, and GP133 proteins were performed with rabbit anti-GP129, -GP131 and -GP133 peptide antibodies and detected with a mouse anti-his antibody. Samples were run on a 10% bis-Tris SDS-PAGE gel. Panels are different film exposures of the same Western. An in-house irrelevant rabbit peptide antibody was used as a negative control.

GPCMV gH, gL, GP129, GP131, and GP133 proteins form a pentameric complex

To determine whether these proteins form a pentameric complex analogous to the HCMV gH/gL/UL128/UL130/UL131 complex, we performed immunoprecipitations from baculovirus-expressed gH, gL, GP129, GP131 and GP133 proteins. First, we immunoprecipitated gH with a mouse monoclonal anti-GPCMV gH antibody (394, generated in-house) or a mouse monoclonal anti-GPCMV gB antibody (29-29) as a species control (Fig. 3C). As expected, gH protein was immunoprecipitated by the anti-GPCMV gH antibody, with relatively minimal gH protein in the negative control lane (Fig. 3C). We also found that gH protein co-immunoprecipitated with gL protein, suggesting formation of a gH/gL heterodimer complex, analogous to that found in HCMV. In addition, gH protein co-immunoprecipitated GP129, GP131 and GP133 proteins, whereas the negative control antibody did not (Fig. 3C).

In addition, we performed the converse experiment by immunoprecipitating the GP129, GP131 and GP133 proteins with the rabbit polyclonal anti-peptide antibodies (anti-GP129, anti-GP131 or anti-GP133). For this experiment, proteins were detected with a mouse anti-his antibody (each protein is his-tagged) instead of the rabbit antibodies due to cross-reactivity of antibody heavy and light chains with the rabbit antibodies used for immunoprecipitation. Furthermore, the anti-gH monoclonal could not be used for Western analysis due to recognition of a non-linear epitope (data not shown). Anti-GP129, anti-GP131 and anti-GP133 antibodies each co-immunoprecipitated gH, GP131 and GP133, whereas a rabbit irrelevant control antibody did not (Fig. 3D). As expected, the anti-GP131 and anti-GP133 immunoprecipitations appeared to pull down more GP131 protein and GP133 protein, respectively (Fig. 3D). Since gL and GP129 share a similar molecular weight (see Fig. 3A), we could not determine which proteins were specifically co-precipitated. Moreover, we could not use the rabbit antibodies to distinguish between gL and GP129, due to co-migration with rabbit antibody light chain. There is a faint band of the same molecular weight as gL/GP129/light chain in the negative control lane; however, this band is present at drastically reduced levels as compared with the anti-GP129, -131, and -133 lanes. Demonstration that gH co-immunoprecipitated gL, GP129, GP131, and GP133, and in addition, GP129, GP131, and GP133 co-immunoprecipitated gH, GP131 and GP133 (and likely gL and/or GP129) strongly suggests complex formation among the components. Furthermore, these results do not rule out sub-complex formation among the components. We were unable to detect the interaction between GP129/GP131/GP133 and gH/gL from infected cells, possibly due to reduced protein levels of GP129/GP131/GP133 during infection (data not shown).

Isolation of a GP129-133 deletion mutant

To understand the function of the gH/gL/GP129/GP131/GP133 complex in GPCMV, we selected for the strain carrying the GP129-133 deletion locus by limiting dilution of the ATCC strain, 22122. In contrast to previously published reports, we isolated the deletion variant in primary guinea pig fibroblast and endothelial cells (Nozawa et al., 2008). The deletion strain was isolated from single plaques on either cell type. This is in contrast to HCMV in which the deletion of this locus occurs only after serial passaging in fibroblast cells but not endothelial cells. Using the P1/P2 primers described previously that flank the GP129-133 locus, we amplified both the 1.6 kb band (wildtype GP129-133 locus) and the 0.4 kb band (deletion of the GP129-133 locus) from virus grown on both cell types and selected for plaques by PCR that only amplified a 0.4 kb band (Fig. 4A and data not shown)(Nozawa et al., 2008). To confirm that we had isolated a deletion, we compared pelleted virus from the parent 22122 strain and the strain isolated via limiting dilution (referred to in Fig. 4A as ΔGP129-133) by SDS-PAGE and Western blot analysis. While an anti-gB antibody was able to react with both the parent 22122 strain and the ΔGP129-133 deletion strain, only the 22122 strain reacted with the anti-GP133 antibody corresponding to a single 15-kD band of

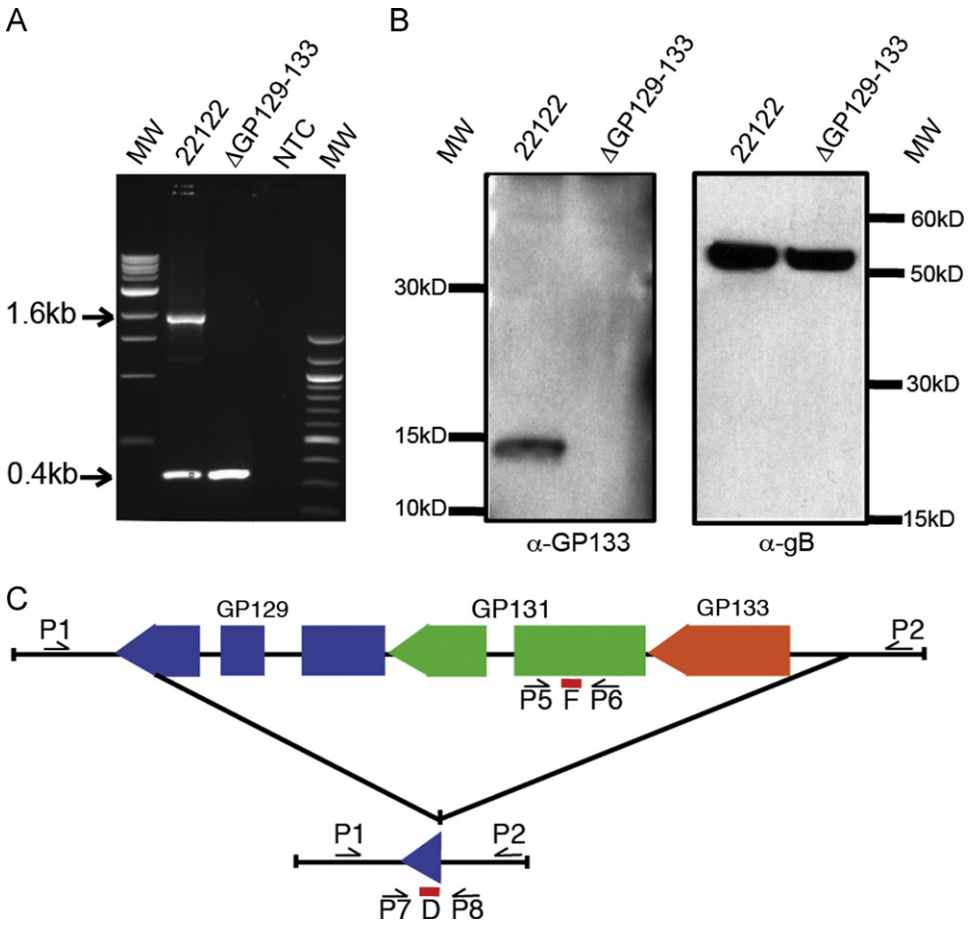

Fig. 4. Isolation and validation of ΔGP129-133 deletion strains. (A) ΔGP129-133 was isolated from primary guinea pig fibroblast cells. PCR reactions were performed with P1 and P2 primers (see panel C). MW = molecular weight, NTC = no template control. (B) Pelleted virus from strain 22122 and the ΔGP129-133 variant was analyzed by Western blot using a mouse anti-gB antibody (29-29) and rabbit anti-GP133 antibody. (C) Boundaries of the deletion clone are shown. P1/P2 primers amplify the region spanning the 1.6 kb region, P5/P6 amplify the wildtype locus by qPCR, and P7/P8 amplify the deletion locus by qPCR. The red bars denote the qPCR probes for the wildtype locus (probe F) and the deletion locus (probe D).

the predicted molecular weight (Fig. 4B). The deletion strain was also confirmed by immunohistochemistry by staining infected gefs using anti-GPCMV gL and anti-GP133 rabbit polyclonal antibodies (Supplemental Fig. 2).

We sequenced the deletion strains isolated on both fibroblasts and endothelial cells and found these sequence deletion boundaries to be consistent with previous reports (Fig. 4C) (Nozawa et al., 2008; Yamada et al., 2009). Similar to published reports, we attempted to make a pure "wildtype" strain (i.e. only contains the 1.6 kb locus) in vitro by limiting dilution followed by plaque purification (Nozawa et al., 2008). We were able to identify several strains that contained only the 1.6 kb locus. However, these purified wildtype strains consistently gave rise to a mixed strain (data not shown). We also attempted to generate a wildtype strain by serial passaging in vivo. Despite 13 serial passages in vivo, the GP129-133 deletion strain could be detected in the salivary gland (Supplementary Fig. 3). These in vitro and in vivo findings strongly suggest genetic instability at this locus, similar to HCMV.

Characterization of the GP129-133 deletion mutant

In HCMV, the UL128-131A deletion strain shows an entry defect in macrophages, endothelial cells, and epithelial cells (Sinzger et al., 2008). To examine whether the GP129-133 deletion strain has a defect in cellular entry, we infected primary endothelial cells with equal numbers of viral genomes (as determined by qPCR) of wildtype and deletion virions. Endothelial cells were infected with 4×10^8 genomes per 2×10^4 cells and fixed at 24 hpi and stained with the monoclonal anti-GPCMV gB antibody (29-29). We found that the deletion strain entered endothelial cells 90% less efficiently than wildtype (Fig. 5A). To determine whether this entry defect was limited to endothelial cells, we performed the same experiment in fibroblast cells. We found that the deletion strain had an entry defect in fibroblast cells to a similar extent as endothelial cells (Fig. 5A). In contrast, the HCMV UL128-131A complex is critical for endothelial entry but dispensable for fibroblast entry. This difference may be due to the functions of the viral glycoproteins or differences between human and guinea pig fibroblast cells. In addition, we found that guinea pig hyperimmune globulin (GP-HIG) neutralized viral entry to an equivalent extent on fibroblasts and endothelial cells (Fig. 5B). This is in contrast to human hyperimmune globulin, which is 100-fold more neutralizing at blocking viral entry into endothelial cells than fibroblasts, due to antibodies that specifically neutralize the HCMV UL128-131A complex (Fouts et al., 2012). Taken together, these data suggest that similar to HCMV 128-131A, the GP129-133 locus plays a role in viral entry and that this role can be extended to fibroblast cells.

To assess if the GP129-133 locus is required for cell-to-cell spread, we compared the ability of the GP129-133 deletion and 22122 strain to spread in fibroblasts. We infected gefs with wildtype at a MOI of 0.1 or with an equivalent number of genomes

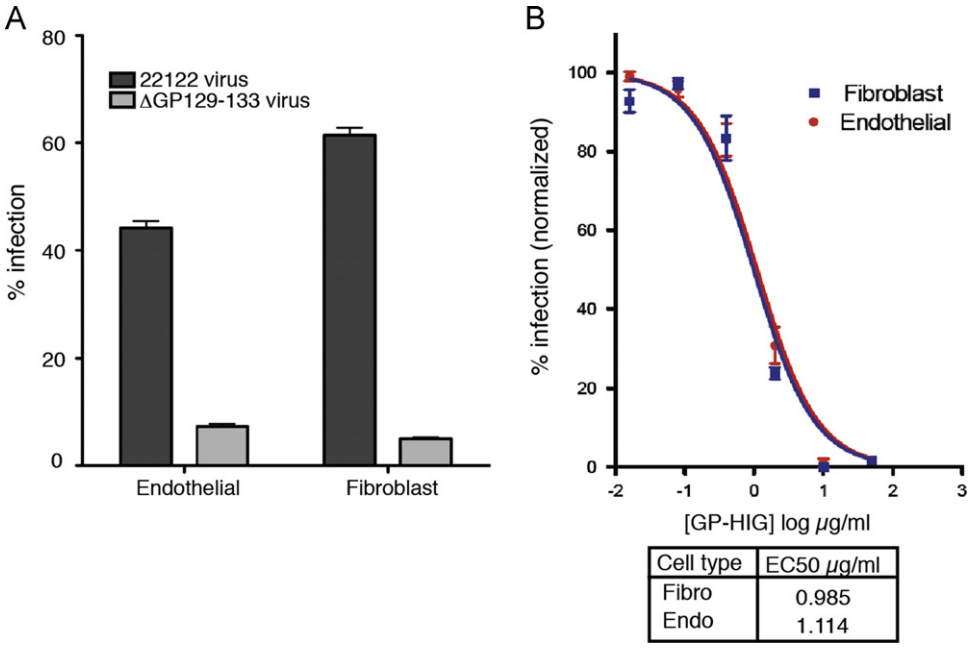

Fig. 5. Evaluation of the ΔGP129-133 virus and guinea pig hyperimmune globulin (GP-HIG) on primary-guinea pig endothelial and fibroblast cells. (A) Comparison of infection of the 22122 strain and the ΔGP129-133 virus. Viral inoculums were equalized by viral genome copy number and stained for anti-GPCMV gB at 24 hpi. (B) Neutralization of the 22122 strain by GP-HIG on both cells types with EC_{50}s shown.

of the GP129-133 deletion strain and measured viral spread by immunofluorescence using an anti-gB antibody (29-29) over the course of 7 days. We found that the GP129-133 deletion strain was initially delayed as compared with wildtype (Fig. 6A, 48–96 hpi). However by day 7, the GP129-133 deletion strain was able to spread to a similar percentage of cells as the 22122 strain (Fig. 6A). Using primer/probe sets specific for the GP129-133 locus (refer to Fig. 4C for primer locations), we determined that the growth was due to the GP129-133 deletion strain rather than contamination from wildtype (Fig. 6B). Thus, the deletion strain is able to spread cell-to-cell with similar kinetics to wildtype (i.e. similar growth curve slopes), but that the growth lag is likely due to an initial defect in entry.

To assess if the GP129-133 locus is required for in vivo spread, we compared the ability of the GP129-133 deletion, 22122 strain, and IVP8 (a virulent strain passaged eight times in vivo) to spread to the salivary gland. To this end, we infected male Hartley guinea pigs (5 animals per group) subcutaneously with each virus stock at 1×10^5 PFU and measured the viral copy number via GP83 (tegument protein) in the salivary glands at day 21 post-infection (Fig. 6C, left panel). Of note, 1×10^5 PFU of the GP129-133 deletion strain contains approximately 10-fold as many genomes as wildtype. As expected, we could detect both the 22122 strain (ave. copy number of 1.4×10^5 genomes/salivary gland (SG)) and IVP8 (ave. copy number of 1.3×10^6 genomes/SG) in the salivary gland. However, the deletion strain failed to spread to the salivary gland, despite an inoculum of 1×10^5 PFU. As expected, the 1.6 kb (wildtype) locus could be amplified (primers P5/P6) from both the 22122- (ave. copy number of 3.6×10^6 genomes/SG) and IVP8-infected samples (ave. copy number of 2.6×10^7 genomes/SG; Fig. 6C, center panel). Despite the failure of the deletion strain to spread in vivo, we could still detect the deletion virus (primers P7/P8) in salivary glands infected with either the 22122 strain (ave. copy number of 2.8×10^5 genomes/SG) or IVP8 (ave. copy number of 5.2×10^4 genomes/SG) (Fig. 6C, right panel). Since the deletion strain fails to spread to the salivary gland, this suggests that the wildtype strain can give rise to the deletion strain in vivo, further suggesting genomic instability at this locus.

Discussion

GPCMV is the closest non-primate relative to HCMV, and bears stronger phylogenetic similarity to primate CMVs than to rodent CMVs (Schleiss et al., 2008). In contrast to the CMVs of other small mammals, GPCMV crosses the placenta, infects the fetus in utero, and produces disease in newborn guinea pigs (Griffith and Aquino-de Jesus, 1991; Schleiss, 2006). The structural similarities between the human and guinea pig placentas, coupled with the relatively long guinea pig gestational period, has made the guinea pig a highly useful model for the study of congenital CMV infection (Schleiss, 2006). Considering the significance of the guinea pig model as the only bona fide small animal CMV congenital infection model, we sought to accomplish the following objectives: (1) introduce a fast, alternative assay to titer viral stocks, (2) introduce the use of guinea pig primary cells for in vitro culture, and (3) characterize the role of the gH/gL/GP129/GP131/GP133 complex in GPCMV entry and spread. Our aim is that these contributions benefit the general study of congenital CMV in addition to the advancement of the guinea pig CMV model.

HCMV entry is facilitated by several entry glycoprotein complexes, with gH/gL/UL128/UL130/UL131A required for viral entry into epithelial cells, endothelial cells, and macrophages, but not fibroblast cells (Hahn et al., 2004; Wang and Shenk, 2005a, 2005b). The neutralizing component of human hyperimmune globulin and the most potent human anti-CMV antibodies described to date are directed against the gH/gL/UL128/UL130/UL131A complex (Fouts et al., 2012; Genini et al., 2011; Macagno et al., 2010; Wang et al., 2011). Despite the biological significance of the HCMV gH/gL/UL128/UL130/UL131A complex, there is little known about an analogous complex in GPCMV.

Here, we have identified the GPCMV homolog of UL131A, called GP133, and shown that it can associate with gH, gL, GP129 and GP131. Although the amino acid similarity between HCMV UL131A and GP133 is low (29%), we conclude that GP133 is the UL131A homolog from the following lines of evidence: (1) both are predicted to contain three conserved alpha-helical domains, in which chimp CMV UL131A contains the highest domain homology and are 32% similar (Fig. 2C), (2) both genes are located in syntenic

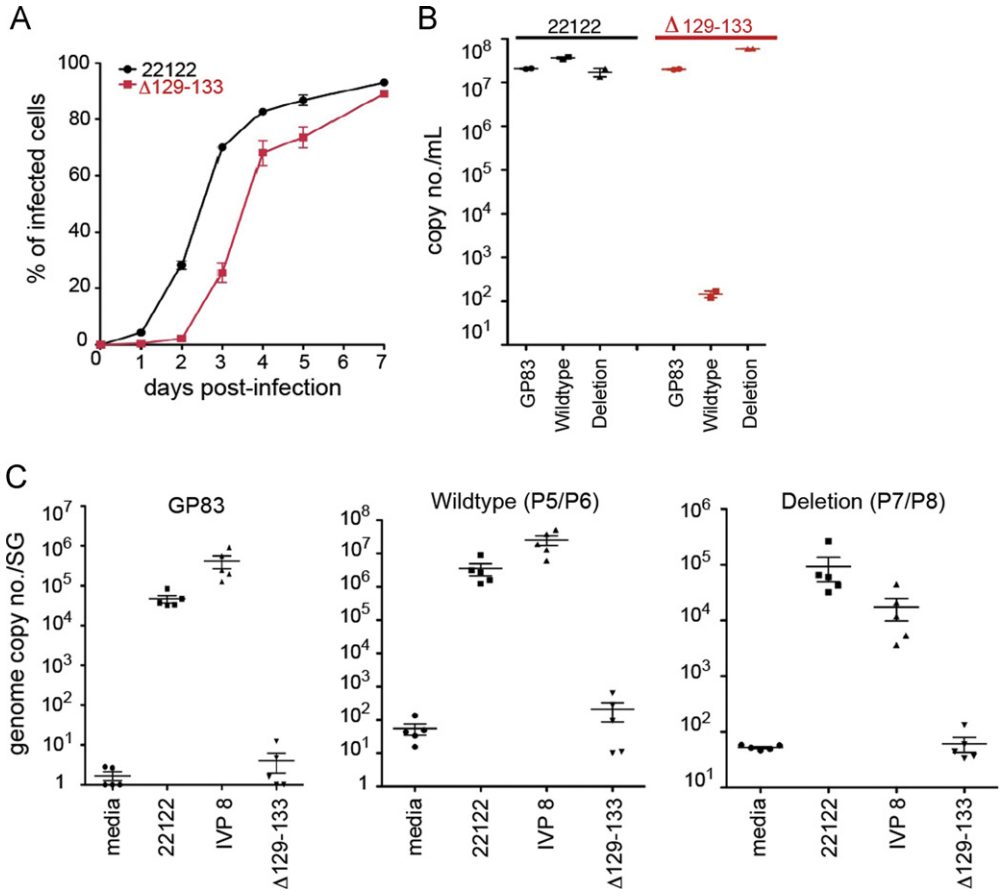

Fig. 6. Comparison of the 22122 strain and the ΔGP129-133 strain in cell-to-cell spread both in vitro and in vivo. (A) In vitro spread assay comparing the growth of the 22122 strain (black) and ΔGP129-133 strain (red) over 7 days. Gefs were infected with wildtype at a MOI of 0.1 or with an equivalent number of genomes of the ΔGP129-133 strain and stained with an anti-GPCMV gB antibody. (B) Quantitative PCR of the released virus at d7 post-infection targeting GP83, the wildtype (P5/P6) locus, and the deletion (P7/P8) locus. (C) Quantitative PCR of virus in salivary glands from guinea pigs infected with 22122, IVP8, or ΔGP129-133 virus targeting GP83, the GP129-133 wildtype locus (P5/P6) and the GP129-133 deletion (P7/P8) locus. Error bars indicate standard error of the mean.

positions in their respective genomes, (3) both GP133 and UL131A are co-cistronic with GP129 and GP131 or UL128 and UL130, respectively, and (4) both GP133 and UL131A proteins form a biochemical complex with gH, gL, and GP129/UL128, and GP131/UL130 (Fig. 3C and D). We recognize the caveats associated with concluding complex formation from baculovirus-expressed proteins, but we were unable to detect the interaction between GP129/GP131/GP133 and gH/gL from infected cells. We believe that this reflects our inability to detect relatively small amounts of GP129/GP131/GP133 protein as compared with gH/gL, as opposed to a lack of an interaction. Our data taken together with demonstration of an analogous complex from HCMV suggests that GPCMV gH/gL/GP129/GP131/GP133 forms a pentamer complex, but does not rule out the formation of sub-complexes.

We have demonstrated that the GPCMV gH/gL/GP129/GP131/GP133 complex is functionally and structurally analogous to the HCMV gH/gL/UL128/UL130/UL131A complex. First, similar to HCMV UL128/UL130/UL131A, we have shown that GPCMV GP129/GP131/GP133 can form a pentamer complex with gH/gL (Fig. 3). Both the GPCMV and the HCMV pentamer complexes contain components with putative chemokine domains (GP129/UL128, GP131/UL130) and a component with a tri-alpha-helical repeat structure (GP133/UL131A). Second, both of these complexes are critical for efficient viral entry into cells. In the case of GPCMV, this complex plays a role in viral entry into both endothelial and fibroblast cells, whereas in HCMV, the complex is dispensable for entry into fibroblasts. This difference is likely due to the functions of the viral glycoproteins but may be due to differences between human and guinea pig fibroblast cells. We acknowledge the limitations of our conclusions from two cell types; however, generating and characterizing additional primary guinea pig cells has proven to be technically challenging. Consistent with GP129-133 proteins playing a role in viral entry, we found that the GP129-133 deletion strain failed to spread in vivo (Fig. 6). Third, both HCMV and GPCMV exhibit genetic instability at this locus. Lab-adapted HCMV strains that have been serially passaged in fibroblasts are functional deletions of the UL128-131A locus (Wang and Shenk, 2005a, 2005b). Similarly in GPCMV, the GP129-133 deletion strain is spontaneously generated from wildtype and perpetuated both in vitro and in vivo passage (Figs. 4, 6 and Supplementary Fig. 3). This study provides evidence for a GPCMV gH/gL/GP129/GP131/GP133 complex and suggests that GPCMV uses entry mechanisms analogous to that of HCMV.

Analysis of the GP129-133 deletion strain suggests that the 129-133 locus, despite its role in entry, is dispensable for in vitro spread, but is required for in vivo spread (Fig. 6). The GP129-133 deletion strain demonstrated an initial lag in growth, but was able to reach wildtype levels of virus after 7 days (Fig. 6A and B). This likely reflects an extracellular entry defect, but not a subsequent defect in cell-to-cell spread, suggesting a gH/gL/GP129-133-independent mechanism for spreading between cells. In vivo, the Δ129-133 strain failed to spread to the salivary gland (Fig. 6C). To reconcile the difference between the in vitro and in vivo results, we propose that the null strain fails to establish infection in the salivary gland due to the requirement for at least two rounds of extracellular entry: one at the injection site, and one at the salivary

gland. In contrast, the wildtype strain can spread to and establish infection in the salivary gland. However, once established in the salivary gland or perhaps at an unspecified intermediate site, the wildtype strain gives rise to the GP129-133 deletion strain in situ, suggesting genetic instability at this locus. This instability may arise due to the gH/gL/GP129-133 complex not being required for spread between cells. This finding is consistent with our observation that plaque-purified wildtype strains (1.6 kb product) regenerate the deletion strain in vitro, making it technically challenging to passage a true wildtype strain. Nozawa et al. (2008) reported the isolation of a true wildtype strain (termed GPCMV/full) after passaging in GPL cells, or a combination of in vivo followed by in vitro passage (Nozawa et al., 2008). One possible difference between these results is that we have used highly characterized primary guinea pig cells for our studies, which may be more relevant to GPCMV biology. Even after 13 serial passages in vivo, we could still detect the deletion of the GP129-133 locus, indicating genetic instability at the GP129-133 locus in vivo and suggesting a growth advantage of the deletion mutant (Supplemental Fig. 3).

We describe in this paper a sensitive, quick method for the detection of GPCMV infection and titering of viral stocks. Despite gB being characterized as a viral late gene, we are able to detect robust gB straining at 24 hpi and found that quantitation of infected cells by anti-gB IFA was equivalent to that determined by $TCID_{50}$. As a result, we were able to reliably use the IFA for titering and adapted this to develop a viral microneutralization assay (Fig. 1 and Supplemental Fig. 4), similar to that currently used for HCMV.

GPCMV is unique in its ability to cross the placenta and cause fetal infection. The guinea pig model has been useful in studying the mechanisms of maternal-fetal transmission (e.g. cell types, route of infection, etc.), in highlighting the importance of pre-conception immunity, and in the development of vaccines. However, our study suggests that the guinea pig model has limited utility to study vaccines and therapeutics that target the HCMV UL128-131A complex, due to the non-analogous roles in entry. There has been a recent focus on the role of HCMV UL128-131A in pre-conception immunity and if antibodies against this complex correlate with fetal protection (Gerna et al., 2008; Wang et al., 2011). Despite these limitations, the guinea pig model can be used to address the protective role of antibodies against other viral entry proteins, such as gB and gH. Ultimately, we hope that this study serves as a technological step forward in the advancement of the guinea pig model, while at the same time deepening the biological understanding of GPCMV.

Materials and methods

Cells, viruses, and animals. Transformed guinea pig lung fibroblasts (GPL, ATCC CCL-158) were cultured in F-12 medium supplemented with 10% fetal bovine serum (FBS). GPLs were initially used to propagate GPCMV as described (Britt and Harrison, 1994). After the generation and extensive characterization of our in-house guinea pig primary fibroblasts, we preferentially used these cells in lieu of the GPLs. Guinea pig embryonic fibroblasts (gefs) were generated from 40-day embryos of Hartley guinea pig purchased from Elm Hill Breeding Labs (Tynsboro, MA and Chelmsford, MA) (Conner, 2001). Gefs were grown in Dulbecco's modified eagle medium (DMEM) containing 10% FBS, penicillin, and streptomycin. Primary lung and aorta endothelial cells were isolated from adult male Hartley guinea pigs, using a protocol adapted from the literature (Sobczak et al., 2010). Primary endothelial cells were sorted with human anti-CD31/PECAM-1 (R&D Systems) and grown in Endothelial Cell Basal Medium-2 (Clonetics) on flasks coated with 1% gelatin. Passaging of the primary endothelial and fibroblast primary cells were limited to up to 6, and 14 passages, respectively.

We created a panel of guinea pig fibroblast-specific (CD90/Thy1, tenascin) and guinea pig endothelial-specific (platelet/endothelial cell adhesion molecule, PCAM-1/CD31, endothelial specific molecule-1, Nos3, VEGF-2, MUC18) markers to characterize these primary cells by quantitative RT-PCR. We based this panel on published markers for human and mouse fibroblast and endothelial cells and the availability of genomic guinea pig sequences (Garlanda and Dejana, 1997; Pilling et al., 2009; Kobayashi et al., 2005). RNA was isolated from guinea pig fibroblast and endothelial cells using the RNeasy Mini Kit (Qiagen) and reverse transcriptase reactions were performed using the High Capacity cDNA reverse transcriptase Kit (Applied Biosystems). Guinea pig specific qPCR primers and probes were designed using the Primer Express Software v3.0 (Applied Biosystems, Supplemental Table 1) with the predicted guinea pig (*Cavia porcellus*) sequences obtained from NCBI via the Guinea Pig Genome Project at the Broad Institute (Cambridge, MA). All Ct values are normalized to guinea pig actin and the normalized fold differences were graphed (Prism, GraphPad Software). qPCR reactions were run in triplicate and error bars indicate standard error of the mean.

GPCMV (strain 22122, American Type Culture Collection) was propagated on gefs. To make viral stocks, cells were infected with the GPCMV strain 22122, at an MOI of 0.01 and harvested between 7 and 9 days post-infection, when ~50% of the cells were detached from the plate. Cells were scraped, and the viral supernatant was spun down to remove cellular debris. Virus was stored in frozen aliquots at −80 °C at 1:1 in 0.2 M sucrose phosphate buffer. To determine the titer of a given stock, an aliquot was thawed and titered. A $TCID_{50}$ assay was initially employed to titer stocks. However this titering technique was augmented by the more facile immunofluoresence assay (IFA) using the mouse monoclonal antibody raised against GPCMV gB (29-29, gift from Bill Britt at the University of Alabama) (Britt and Harrison, 1994). The cells were fixed in ethanol at 24 hpi, blocked with PBS containing 2% bovine serum albumin (BSA), and stained with anti-gB (29-29) at 2 μg/mL, anti-mouse AlexaFluor 488 and DAPI stain (Invitrogen). The cells were imaged and scored using the Image Express Micro and MetaXpress software (Molecular Devices). IFA at 24 hpi gave comparable titers to $TCID_{50}$ at 14 days post-infection. Viral stocks typically had titers of 10^5–10^6 PFU/ml on fibroblast and endothelial cells.

For Western blotting, virus was partially purified and pelleted from the supernatant of infected cells. The medium was layered over a sorbitol cushion (20% D-sorbitol in PBS) and virus was pelleted by ultracentrifugation (22,000 rpm, 90 min, SW28 Beckman rotor). Viral pellets were resuspended in lysis buffer (50 mM Tris, 150 mM NaCl, 0.1% SDS, 1% NP-40, Complete, Mini protease inhibitor cocktail tablet from Roche) and subsequently prepared for SDS/PAGE-Western blot analysis.

In vitro generated viral stocks were passaged in vivo by the following method: adult male Hartley guinea pigs (Elm Hill Breeding Labs, Tynsboro and Chelmsford, MA) were infected subcutaneously with 10^5 PFU of tissue culture-derived virus stock. After 21 days of infection, the salivary gland was removed, homogenized, sonicated, clarified and used for re-infection as previously described (Hartley et al., 1957). After each passage, virus was stored in frozen aliquots at −80 °C at 1:1 in 0.2 M sucrose phosphate buffer at 10^5 PFU/ml. Before their use in the study, all animals were tested for GPCMV antibodies by neutralization assay and only GPCMV-free animals were used. All guinea pigs were housed under conditions approved by the American Association of Accreditations of Laboratory Animal Care Committee.

Guinea pig hyperimmune globulin (GP-HIG). GP-HIG was produced by infecting 10 GPCMV-free adult Hartley male guinea pigs subcutaneously with tissue-culture derived GPCMV at 10^6 PFU/animal (1 ml total volume). Antibody responses were boosted by two subsequent injections at 3-week intervals with 10^6 PFU/animal. Prior to each injection, serum was collected and tested for neutralization with GPCMV. Terminal bleeds from infected animals were taken at 9-weeks post the initial injection, pooled, and affinity purified for IgG. In a separate experiment, non-immune negative control serum was generated from 10 uninfected Hartley male guinea pigs and affinity purified for IgG. The affinity purified GP-HIG and non-immune IgG was tested for neutralization activity on primary guinea pig fibroblast and endothelial cells.

Neutralization assays. GPCMV neutralization assays were based on assays from the HCMV literature (Abai et al., 2007). Briefly, guinea pig hyperimmune globulin (GP-HIG) or non-immune IgG was serially diluted in complete DMEM and mixed with virus diluted in DMEM such that the final virus concentration resulted in approximately one infectious virus per cell (MOI = 1) when mixed with media. Antibody and virus were mixed and incubated at 37 °C for 1 h prior to incubation for 24 h on a confluent monolayer of cells. At 24 hpi, cells were fixed and stained with the anti-GPCMV gB antibody (29-29) as described above. Data from duplicate wells containing a given antibody concentration were averaged and compared with infection in the absence of antibody, which was set to 100%. Data were graphed using Prism (GraphPad Software; La Jolla, CA), and EC_{50} values were calculated from best-fit curves using Prism EC_{50}-curve fitting algorithm.

Peptide antibodies. Rabbit polyclonal antibodies were generated to GPCMV gH, gL, GP129, GP131 and GP133 for biochemical analyses and immunohistochemistry. The following rabbit polyclonal antibodies were generated: gH (raised against SPQELYNWAPHVSSAGLTMQEMFTPCSGSGRRDYTE), gL (raised against CVRRILYQASLSGPHRDAPIHNYLNRDLS), GP129 (raised against CSSKDRRVQHSTTSND), GP131 (raised against CYYPSTPIPKSFVKHV), and GP133 (raised against CENQLAHYILKTIVLTHHRR) (YenZym Antibodies, South San Francisco). Antibodies were affinity-purified on peptide.

Immunohistochemistry. Guinea pig fibroblast cells were infected at an MOI of 1 for 24 h and cell pellets were immersed for 24 h in neutral-buffered formalin at ambient temperature, paraffin-embedded, then sectioned at 4 μm and mounted on glass slides. Slides were stained with anti-GP gL and anti-GP133 antibodies on a Ventana Discovery XT Autostainer, with Ventana CC1 standard digestion and Ventana Rabbit OmniMap DAB detection. Images were captured on a Nikon E800 microscope equipped with a Leica DFC500 camera and Leica Application Suite software (v 3.6.0). Digital magnification and image compression was performed in Adobe Photoshop CS3 (v 10.0.1).

Cloning, sequencing, and annotation. GPCMV cDNA was generated from a pool of poly(A) RNA purified from GPCMV-infected cells, and the entire locus was amplified using primers encompassing the entire 1.6 kb region (129rev CCTGTATCGGCGAAAGACA), 133 for (ATGTTTTGGCGTCTTGTATATGTCTA) based on genomic sequence from the literature (Nozawa et al., 2008). The PCR reaction yielded three products that were individually cloned into the TOPO vector (Invitrogen) and sequenced. The PCR product did not contain sequences corresponding to gp130 and gp134. The locus is expressed from the Crick (negative) strand as a single mRNA. Sequencing and comparison of the cDNA and genomic DNA sequences confirmed that GP129 and GP131 are spliced and GP133 is unspliced. Secondary structure predictions were made using Protein Structure Prediction (PELE) on Biology Workbench (Subramaniam, 1998). The chimpanzee CMV (CCMV, Panine herpesvirus 2) UL131A sequence (accession no. AF480884) was used in the alignment in Fig. 2C.

Baculovirus production of GPCMV glycoproteins. Recombinant plasmids made from cDNA clones were used to subclone GPCMV gH, gL, GP129, GP131, and GP133 containing C-terminal His tags. For expression in baculovirus of gH, the transmembrane domain was eliminated to maximize secretion into the media. Native signal sequences were removed and replaced with the insect signal sequence. In brief, *Spodoptera frugiperda* (Sf9) and *Trichloplusia ni* (Tni) cells were obtained from Expression Systems LLC. Cells were maintained in ESF921 complete insect media in shake flasks. For generation of recombinant baculovirus, Tni cells were transfected with plasmid DNA using Baculogold cotransfection reagent (BD Biosciences). Stocks of recombinant baculovirus expressing GPCMV glycoproteins were passaged 3 times in Sf9 cells and stored in 2% HIFBS. For protein expression, Tni cells in shake flasks or wave bioreactors were infected at a density of 2×10^6 cells/ml and co-infected at an MOI of 1 in equal ratios. Cells were incubated at 37 °C and supernatant was harvested at 72 h post infection. Protein was then purified over nickel resin and analyzed by SDS-PAGE and Western blot. Standard Western blotting was performed using the rabbit polyclonal antibodies and a mouse anti-his monoclonal antibody (Clontech).

Detection of GPCMV glycoproteins in GPCMV-infected fibroblast cells. Confluent fibroblast cells were infected at an MOI of ~2 and cell lysates were made at 48 hpi in 1× TBS buffer (pH 7.5) supplemented with 1 mM $MgCl_2$, 50 μM $CaCl_2$, Complete, EDTA-free Mini protease inhibitor cocktail tablet from Roche, and 1% Triton X-100. Western blot analysis was performed using the rabbit peptide antibodies. An uninfected cell lysate was included as a negative control.

Co-immunoprecipitations of the baculovirus-produced GPCMV pentamer complex. Immunoprecipitation experiments were performed with a mouse monoclonal anti-guinea pig gH antibody (394, generated in-house) and rabbit peptide antibodies against GP129, GP131 and GP133 (described above). The corresponding negative species control antibodies were a mouse monoclonal anti-GPCMV gB antibody (29-29) and an irrelevant rabbit anti-peptide control (derived in-house), respectively. Purified gH, gL, GP129, GP131, and GP133 protein was incubated with antibody in TBS buffer overnight at 4 °C, complexed with protein A/G sepharose beads (Pierce) for 1 h, and washed three times in TBS buffer containing 1% Triton-X100. The boiled samples were analyzed by SDS-PAGE/Western blot analysis with the affinity-purified rabbit polyclonal antibodies or a mouse-anti-his antibody (Clontech).

Preparation of GPCMV DNA from salivary gland. Guinea pig salivary gland tissue was homogenized with gentleMACS Dissociator (MACS Miltenyi Biotec) in 5 mL of PBS. Salivary gland homogenates were centrifuged to remove debris. Two hundred microliter of the homogenized tissue was used for DNA isolation with Qiagen DNeasy blood and tissue kit. DNA samples were analyzed using quantitative PCR.

PCR assays. The copy number of GPCMV DNA was calculated using a standard curve prepared from a plasmid containing the target sequence, GP83 (tegument), by quantitative PCR. To normalize the GPCMV DNA copy numbers in a single cell, copy numbers of the guinea pig β-actin gene were determined by qPCR. TaqMan primer and probe sets for GP83 and guinea pig β-actin were designed as previously described (Katano et al., 2007; Nozawa et al., 2008). Zero Blunt PCR TOPO plasmids (Invitrogen) containing one copy of the GP83 or guinea pig actin gene were used to construct standard curves for quantification. Ten-fold serial dilutions ranging from 10^8 to 100 copies per 25 μl reaction volume were used. Standard curves with > 95% amplification were used for determining viral copy number.

To examine the 1.6 kb locus, two PCR approaches were taken as previously described (Nozawa et al., 2008). First, standard PCR for detection of the 1.6 kb locus was performed using primers P1 and

P2 that span the 1.6 kb region. Second, to quantify the amount of the 1.6 kb (full-length) and the 0.4 kb (deletion) in each sample, qPCR assays were adapted from the literature (Nozawa et al., 2008). The first primer/probe set targeted a sequence within the GP131 gene, internal to the 1.6 kb region, (P5, ATAAACGTCGCAGTCCAACGTT, P6, CGTCCTTCTTGTGGCATTATACG probe F, CACCGTCTTTCATCCGT), and the second set amplified the new junction created upon the deletion of the 1.6 kb region (P7, CGTGTATGAAAATGTGTGGACTGA, P8, TAGAAAGGTGCATAATAAACCGTTGA, probe D, TAGAAACGCCC-junction-AGCATCTTGG). To determine the copy number, the 1.6 kb and 0.4 kb PCR products generated from the conventional PCR using P1/P2 were cloned into Zero Blunt PCR TOPO vectors (Invitrogen) and used to make standard curves. See Fig. 4C for the primer and probe positions.

Acknowledgments

We would like to thank Bill Britt (University of Alabama) for his generous gift of the mouse anti-GPCMV gB monoclonal antibody, 29-29. We thank Sharookh Kapadia for assistance with qPCR and Dave Lee for isolation of guinea pig endothelial cells. We would like to thank Katharina Stengel for baculovirus protein purifications and biochemistry assistance. Thanks to Rajesh Vij and Jo-AnneHongo for generation of the gH antibody. Special thanks to Mark Schleiss for meaningful discussions.

Appendix A. Supporting information

Supplementary data associated with this article can be found in the online version at http://dx.doi.org/10.1016/j.virol.2013.03.008.

References

Abai, A.M., Smith, L.R., Wloch, M.K., 2007. Novel microneutralization assay for HCMV using automated data collection and analysis. J. Immunol. Methods 322, 82–93.

Brady, R.C., Schleiss, M.R., 1996. Identification and characterization of the guinea-pig cytomegalovirus glycoprotein H gene. Arch. Virol. 141, 2409–2424.

Britt, W.J., Harrison, C., 1994. Identification of an abundant disulfide-linked complex of glycoproteins in the envelope of guinea pig cytomegalovirus. Virology 201, 294–302.

Conner, D.A., 2001. Mouse embryo fibroblast (MEF) feeder cell preparation. Curr. Protoc. Mol. Biol. 51, 23.2.1–23.2.7.

Fouts, A.E., Chan, P., Stephan, J.P., Vandlen, R., Feierbach, B., 2012. Antibodies against the gH/gL/UL128/UL130/UL131 complex comprise the majority of the anti-CMV neutralizing antibody response in CMV-HIG. J. Virol. 13, 7444–7447.

Garlanda, C., Dejana, E., 1997. Heterogeneity of endothelial cells. Specific markers. Arterioscler Thromb Vasc Biol 17, 1193–1202.

Genini, E., Percivalle, E., Sarasini, A., Revello, M.G., Baldanti, F., Gerna, G., 2011. Serum antibody response to the gH/gL/pUL128-131 five-protein complex of human cytomegalovirus (HCMV) in primary and reactivated HCMV infections. J Clin Virol 52, 113–118.

Gerna, G., Sarasini, A., Patrone, M., Percivalle, E., Fiorina, L., Campanini, G., Gallina, A., Baldanti, F., Revello, M.G., 2008. Human cytomegalovirus serum neutralizing antibodies block virus infection of endothelial/epithelial cells, but not fibroblasts, early during primary infection. J Gen Virol 89, 853–865.

Griffith, B.P., Aquino-de Jesus, M.J., 1991. Guinea pig model of congenital cytomegalovirus infection. Transplantation Proceedings 23, 29–31, Discussion 31.

Hahn, G., Revello, M.G., Patrone, M., Percivalle, E., Campanini, G., Sarasini, A., Wagner, M., Gallina, A., Milanesi, G., Koszinowski, U., Baldanti, F., Gerna, G., 2004. Human cytomegalovirus UL131-128 genes are indispensable for virus growth in endothelial cells and virus transfer to leukocytes. J. Virol. 78, 10023–10033.

Hartley, J.W., Rowe, W.P., Huebner, R.J., 1957. Serial propagation of the guinea pig salivary gland virus in tissue culture. Proceedings of the Society for Experimental Biology and Medicine, 96, pp. 281–285.

Kanai, K., Yamada, S., Yamamoto, Y., Fukui, Y., Kurane, I., Inoue, N., 2011. Re-evaluation of the genome sequence of guinea pig cytomegalovirus. J Gen Virol 92, 1005–1020.

Katano, H., Sato, Y., Tsutsui, Y., Sata, T., Maeda, A., Nozawa, N., Inoue, N., Nomura, Y., Kurata, T., 2007. Pathogenesis of cytomegalovirus-associated labyrinthitis in a guinea pig model. Microbes Infect. Inst. Pasteur 9, 183–191.

Kobayashi, M., Inoue, K., Warabi, E., Minami, T., Kodama, T., 2005. A simple method of isolating mouse aortic endothelial cells. J Atheroscler Thromb 12, 138–142.

Macagno, A., Bernasconi, N.L., Vanzetta, F., Dander, E., Sarasini, A., Revello, M.G., Gerna, G., Sallusto, F., Lanzavecchia, A., 2010. Isolation of human monoclonal antibodies that potently neutralize human cytomegalovirus infection by targeting different epitopes on the gH/gL/UL128-131A complex. J. Virol. 84, 1005–1013.

Malkowska, M., Kokoszynska, K., Dymecka, M., Rychlewski, L., Wyrwicz, L.S., 2013. Alphaherpesvirinae and Gammaherpesvirinae glycoprotein L and CMV UL130 originate from chemokines. Virol. J. 10, 1.

Nozawa, N., Yamamoto, Y., Fukui, Y., Katano, H., Tsutsui, Y., Sato, Y., Yamada, S., Inami, Y., Nakamura, K., Yokoi, M., Kurane, I., Inoue, N., 2008. Identification of a 1.6 kb genome locus of guinea pig cytomegalovirus required for efficient viral growth in animals but not in cell culture. Virology 379, 45–54.

Ogawa, H., Suzutani, T., Baba, Y., Koyano, S., Nozawa, N., Ishibashi, K., Fujieda, K., Inoue, N., Omori, K., 2007. Etiology of severe sensorineural hearing loss in children: independent impact of congenital cytomegalovirus infection and GJB2 mutations. J. Infect. Dis. 195, 782–788.

Paglino, J.C., Brady, R.C., Schleiss, M.R., 1999. Molecular characterization of the guinea-pig cytomegalovirus glycoprotein L gene. Arch. Virol. 144, 447–462.

Pass, R.F., 2002. Cytomegalovirus infection. Pediatr. Rev. 23, 163–170.

Pilling, D., Fan, T., Huang, D., Kaul, B., Gomer, R.H., 2009. Identification of markers that distinguish monocyte-derived fibrocytes from monocytes, macrophages, and fibroblasts. PLoS One 4, e7475.

Powers, C., Fruh, K., 2008. Rhesus CMV: an emerging animal model for human CMV. Med. Microbiol. Immunol. 197, 109–115.

Ryckman, B.J., Rainish, B.L., Chase, M.C., Borton, J.A., Nelson, J.A., Jarvis, M.A., Johnson, D.C., 2008. Characterization of the human cytomegalovirus gH/gL/UL128-131 complex that mediates entry into epithelial and endothelial cells. J. Virol. 82, 60–70.

Schleiss, M.R., 2002. Animal models of congenital cytomegalovirus infection: an overview of progress in the characterization of guinea pig cytomegalovirus (GPCMV). J. Clin. Virol. 25 (Suppl 2), S37–49.

Schleiss, M.R., 2006. Nonprimate models of congenital cytomegalovirus (CMV) infection: gaining insight into pathogenesis and prevention of disease in newborns. ILAR J. 47, 65–72.

Schleiss, M.R., 2007. Prospects for development and potential impact of a vaccine against congenital cytomegalovirus (CMV) infection. J. Pediatr. 151, 564–570.

Schleiss, M.R., McGregor, A., Choi, K.Y., Date, S.V., Cui, X., McVoy, M.A., 2008. Analysis of the nucleotide sequence of the guinea pig cytomegalovirus (GPCMV) genome. Virol. J. 5, 139.

Sinzger, C., Digel, M., Jahn, G., 2008. Cytomegalovirus cell tropism. Curr. Top. Microbiol. Immunol. 325, 63–83.

Sobczak, M., Dargatz, J., Chrzanowska-Wodnicka, M., 2010. Isolation and culture of pulmonary endothelial cells from neonatal mice. J. Vis. Exp. 46, 2316.

Spaete, R.R., Thayer, R.M., Probert, W.S., Masiarz, F.R., Chamberlain, S.H., Rasmussen, L., Merigan, T.C., Pachl, C., 1988. Human cytomegalovirus strain Towne glycoprotein B is processed by proteolytic cleavage. Virology 167, 207–225.

Straschewski, S., Patrone, M., Walther, P., Gallina, A., Mertens, T., Frascaroli, G., 2011. Protein pUL128 of human cytomegalovirus is necessary for monocyte infection and blocking of migration. J. Virol. 85, 5150–5158.

Subramaniam, S., 1998. The Biology Workbench—a seamless database and analysis environment for the biologist. Proteins 32, 1–2.

Wang, D., Shenk, T., 2005a. Human cytomegalovirus UL131 open reading frame is required for epithelial cell tropism. J. Virol. 79, 10330–10338.

Wang, D., Shenk, T., 2005b. Human cytomegalovirus virion protein complex required for epithelial and endothelial cell tropism. Proc. Natl. Acad. Sci. USA 102, 18153–18158.

Wang, D., Li, F., Freed, D.C., Finnefrock, A.C., Tang, A., Grimes, S.N., Casimiro, D.R., Fu, T.M., 2011. Quantitative analysis of neutralizing antibody response to human cytomegalovirus in natural infection. Vaccine 29, 9075–9080.

Wyrwicz, L.S., Rychlewski, L., 2007. Herpes glycoprotein gL is distantly related to chemokine receptor ligands. Antiviral Res. 75, 83–86.

Yamada, S., Nozawa, N., Katano, H., Fukui, Y., Tsuda, M., Tsutsui, Y., Kurane, I., Inoue, N., 2009. Characterization of the guinea pig cytomegalovirus genome locus that encodes homologs of human cytomegalovirus major immediate-early genes, UL128, and UL130. Virology 391, 99–106.